PHYSICAL REVIEW E VOLUME 58, NUMBER 5 NOVEMBER 1998

Biorthogonal decomposition analysis and reconstruction of spatiotemporal chaos generated by coupled wakes

J. F. Ravoux and P. Le Gal
Institut de Recherche sur les Phénomènes Hors Equilibre, UM 6594, Université d'Aix-Marseille I & II, CNRS, 12 Avenue Général Leclerc, 13003 Marseilles, France

(Received 20 February 1998; revised manuscript received 8 September 1998)

Very often in hydrodynamics, the description of the complexity of flows can only be achieved by the use of simple models. These models, obtained usually by phenomenological arguments, need in general the knowledge of some parameters. The challenge is then to determine the values of these parameters from experiments. Here, our concern is the description of a coupled wakes experiment using a complex Ginzburg-Landau equation (GLE). Our analysis is based on a proper decomposition of experimental spatiotemporal chaotic flow fields, followed by a projection of the GLE onto the proper directions. We show that our method is able to recover the parameters of the model which permit us to reconstruct the spatiotemporal chaos observed in the experiment. As it is based on a general projection principle, this method is general and could be applied to other systems. [S1063-651X(98)51611-X]

PACS number(s): 47.27.Vf, 05.45.+b, 47.35.+i, 47.52.+j

INTRODUCTION

It is known from experimental studies [1] and numerical simulations [2] that the wakes of bluff bodies placed side by side can interact and create a large variety of phenomena. In particular, the acoustic mode where all the wakes oscillate in phase, and the optical mode where all the wakes oscillate in phase opposition, are obtained for, respectively, strong and weak coupling [3]. In the case of interest here, we analyze the space-time chaos created by 16 wakes in interaction in the narrow window of intermediate range of coupling. This spatiotemporal chaos is characterized by randomly generated space-time dislocations which are associated with wakes extinctions or amplitude holes [4,5]. Figure 1 (top) presents a snapshot of the coupled wakes that are visualized by dye injection through small holes drilled in the middle plane of each cylinder. Amplitude holes and phase jumps of π are particularly visible on this image (wake numbers 6 and 15). The cylinders possess a length of 200 mm and a diameter of 2 mm. They are rigidly maintained in the wall of a water tunnel. The distance separating each cylinder axes is equal to four times their diameter. The experiments are run at a Reynolds number of 80. They are recorded via a standard video system and a frame grabber driven by a microcomputer. In particular, we can record a unique video line at the video frequency (25 Hz) and gather these lines to build space-time diagrams (452 time steps$\times$16 space positions) that represent the dynamics of the family of wakes. The acquisition line is situated 12 mm downstream the row of cylinders and the displacements of the dye streaks are recorded as a function of time. The amplitude of the signal is normalized by the standard deviation of the total signal, and the time unit is 0.04 s. Figure 1 (bottom) shows such an observation window where the intermittency of amplitude holes is visible.

DATA ANALYSIS

The Bénard–von Karman wake of a cylinder placed in a flow appears via a Hopf bifurcation. The oscillating flow can then be modeled by a Stuart-Landau equation [6,7]. Thus, the coupled oscillators model that can be used to study the flow downstream the row of cylinders is a discrete version of the generalized Ginzburg-Landau equation (GLE) [8,4],

$$d_tA_i(t)=(a_r+ja_i)A_i(t)+(g_r+jg_i)[A_{i+1}(t)+A_{i-1}(t)-2A_i(t)]-(l_r+jl_i)|A_i(t)|^2A_i(t). \tag{1}$$

The associated boundary conditions are $A_0(t)=A_{17}(t)=0$, where $A_i(t)$ is the complex amplitude of the wake of index i. Note that it has been shown by a previous experiment realized on a pair of wakes [9] that the wakes are de-

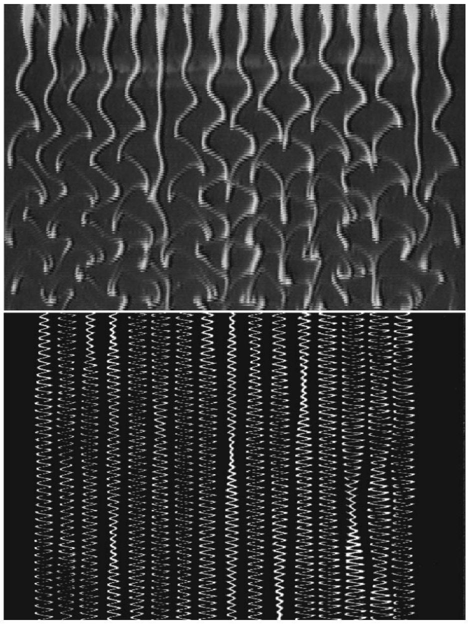

FIG. 1. Snapshot of the 16 coupled wakes (top). Space-time diagram (bottom), time is running downward.

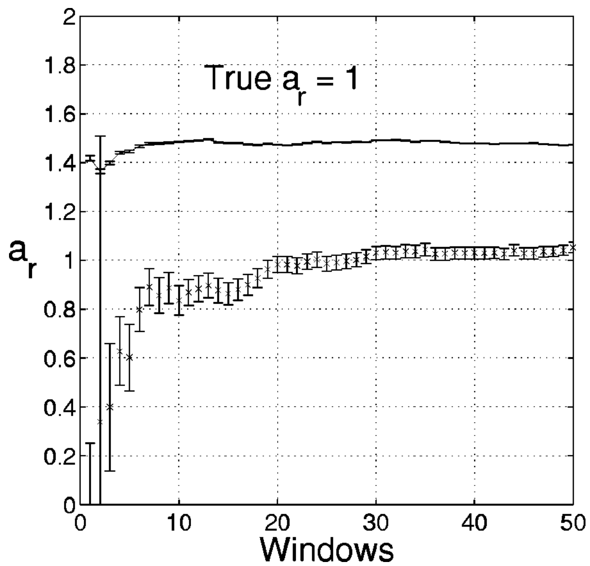

FIG. 2. Comparison of convergence results between the direct method (−) and the dispersion relation method (×).

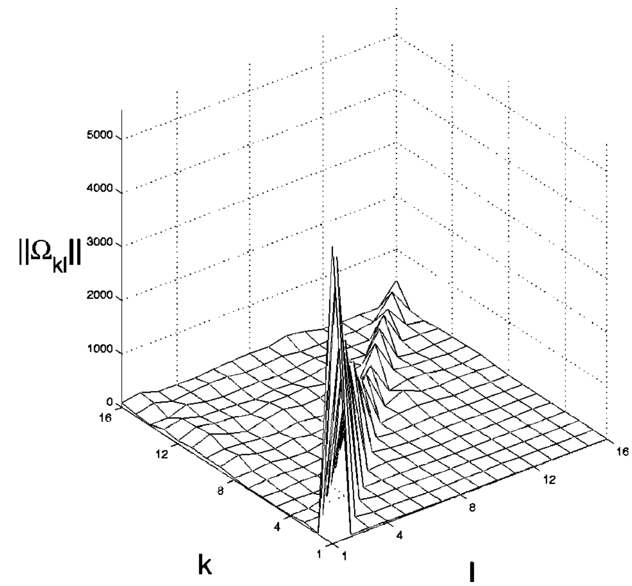

FIG. 3. Three-dimensional representation of the matrix Ω, calculated from the experimental data.

coupled when the distance separated their axes, is larger than six times their diameter. This is the reason why an interaction at first neighbors only can be considered.

The three complex coefficients a, g, and l, appearing in the GLE (1), determine the wakes dynamics and their recovering from experimental spatiotemporal chaotic measurements represents a real challenge of data analysis. In this study, we develop a technique proposed by [5] that permits us to measure the values taken by these parameters. Two methods based on the biorthogonal decomposition [10] will be used. The first one (called the direct method) analyzes directly the spatiotemporal data series similarly to what was done on the same problem in [11] or in a surface wave study [13]. As we will see further, this direct method suffers a lot from the presence of noise.

On the contrary, the second method is based on the characterization of a generalized dispersion relation defined by a Galerkin projection as defined in [5]. We will focus here on this second method, which permits a better reconstruction of the data. To illustrate this point, we present in Fig. 2 a comparison of the determination of the real part of the linear coefficient a_r from synthetic data. In this case, the true value of a_r is equal to 1. A numerical simulation of the GLE is realized and a 10% Gaussian noise is added, simulating an eventual experimental noise. As can be seen, the direct method, which essentially consists of an inversion problem, cannot recover the exact value of the parameter. The observed convergence to a false asymptotic value with the increasing number of windows is due to the presence of noise and may explain the difficulties encountered in previous studies [13]. The second method, whose results are also shown in Fig. 2, is presented in the following. Although it possesses a less good rate of convergence, it predicts the true value of the parameter with an accuracy of 5% (instead of 50% for the direct method). The same observation can be made on the determination of the other parameters and thus definitively sets our choice on the dispersion relation method. Moreover, it needs a smaller volume of data and consequently is much faster than the direct one.

As the GLE is a complex model, the first step of the method consists of complexifying the experimental data. This is obtained by a classical procedure, using the Hilbert Transform. Then, the $N=16$ proper modes of the complex field $A_{ti}=A_i(t)$ are calculated by diagonalization of the temporal correlation (16×16) matrix and by the use of the projection relation [10]

$$A_{ti}=\sum_{k=1}^{N} \alpha_k \psi_k(t)\overline{\phi_k}(i), \tag{2}$$

where the overbar designs the complex conjugation, ψ_k the temporal mode, and ϕ_k the spatial mode associated with the eigenvalue α_k. According to the time, space, and nonlinear operators of Eq. (1), the following (452×16) matrices are previously built from A:

$$D_{ti}=\frac{A_{t+1i}-A_{ti}}{\Delta t},$$

$$\Delta_{ti}=A_{ti+1}+A_{ti-1}-2A_{ti},$$

$$N_{ti}=|A_{ti}|^2A_{ti},$$

where Δt is the time unit given by the video acquisition rate. When Eq. (1) is projected onto the proper orthogonal decomposition modes, the following (16×16) matrices appear:

$$\Omega_{kl}=((D_{ti}\Phi_{il})^*\psi_{tk})^*, \quad L_{kl}=((A_{ti}\Phi_{il})^*\psi_{tk})^*,$$

$$\kappa_{kl}=((\Delta_{ti}\Phi_{il})^*\psi_{tk})^*, \quad \Gamma_{kl}=((N_{ti}\Phi_{il})^*\psi_{tk})^*,$$

where the inner product is the usual product of complex matrices with the complex conjugate of the transpose of any matrix noted by an asterisk. The dispersion relation linking modes l and k can then be written as

$$\Omega_{kl}=aL_{kl}+g\kappa_{kl}-l\Gamma_{kl}. \tag{3}$$

Figure 3 presents the absolute value of the elements of the

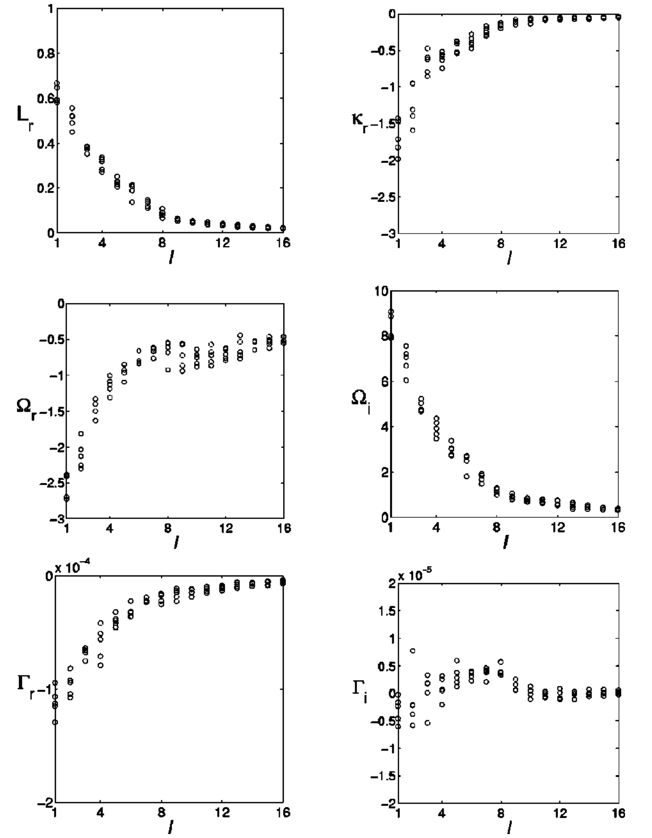

FIG. 4. Experimental data: Evolution versus index l of the diagonal elements of the matrices Ω, L, κ, and Γ (arbitrary units).

matrix Ω that are calculated here for one experimental observation window of 16×452 data points. As can be seen, the matrix Ω is almost diagonal. The same observation being made on the other matrices, the only modes $k=l$ will be considered in the following.

A good representation of the spatiotemporal dynamics is achieved when considering these diagonal elements as a function of the mode index l. These ''spectra'' represent in fact the signature of the experimental spatiotemporal signals. Therefore, we emphasize the fact that, contrary to what was done in [11], our intention is not to reconstruct precisely a particular window among the 50 which are analyzed, but to obtain the parameters of the GLE which will permit us to recover the ''spectra.'' Figure 4 gives the shape of these spectra for five superimposed different experimental observation windows. Note that, as mentioned in [5], the matrix κ is self-adjoint and the imaginary parts of its diagonal elements are null.

Therefore, the determination of the coefficients a, g, and l lies on the inversion of this dispersion relation (3), where the matrices Ω, L, κ, and Γ are obtained from experimental data. The method had been first successfully tested on simulated data processed by the GLE, with or without added noise. Then and to annihilate the experimental noise, we analyze statistically about 50 windows of 452×16 data points. Moreover, to decrease the influence of experimental noise, the last four modes, where the signal to noise ratio is observed to be less than 50%, will also be neglected in the inversion process.

The parameters are obtained by a normal equations resolution [13]. This least-square method consists of the representation of data on maximum correlation directions. The examination of the relative standard deviation associated with these directions allows us to withdraw uncorrelated data [15], which are essentially due to the experimental and video data processing noise. Here the relative standard deviation corresponding to these irrelevant data is about 0.14%. The coefficients a, l, and g take the following values:

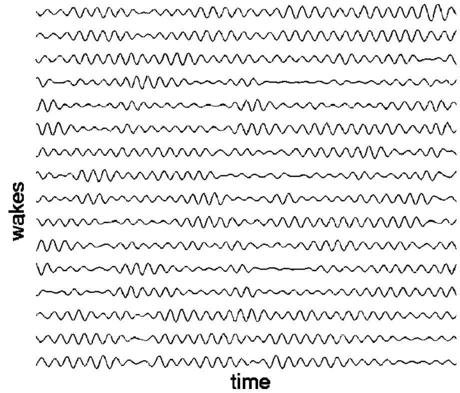

FIG. 5. Space-time diagram of the 16 simulated coupled wakes with the coefficients obtained from the experiment.

$$a_r=-0.0534[(t)^{-1}],\quad a_i=0.4747[(t)^{-1}],$$

$$g_r=-0.2396[(t)^{-1}],\quad g_i=-2.7018[(t)^{-1}],$$

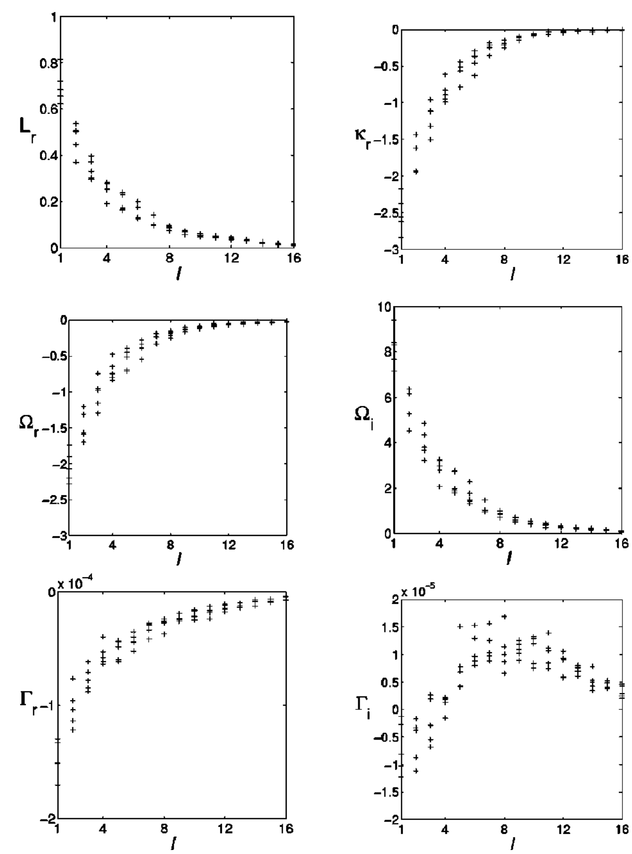

FIG. 6. Evolution vs index l of the diagonal elements of the matrices Ω,L,κ,Γ obtained from five windows of the 16 simulated coupled wakes with the coefficients obtained from the experiment.

$$l_r = 0.0567[(t)^{-1}(A)^{-2}], \quad l_i = -0.0795[(t)^{-1}(A)^{-2}].$$

In fact, the relevant parameters of Eq. (1) are normalized and deduced from the latter, $\eta = g_r/a_r$, $c_1 = g_i/g_r$ and $c_2 = l_i/l_r$. They can be compared to the ones determined in [14] and [12],

$$\eta = 4.48, \quad c_1 = 11.27, \quad c_2 = -1.40.$$

Whereas the parameter c_2 takes exactly the value obtained in [14], there are noticeable differences with the results presented in [12].

RECONSTRUCTION AND CONCLUSION

Using these values, the GLE model is simulated with an Euler integration scheme and shows in Fig. 5, a good agreement with the observed spatiotemporal chaotic behavior. In particular, the extinctions of oscillators are recovered. To obtain a crude comparison between the simulation and the experiment, the largest positive Lyapunov exponent can be estimated in each case. The experimental one is equal to 0.17 ± 0.02, which can be compared to the slightly smaller one 0.13 ± 0.02, calculated from the numerical simulation.

To analyze more specifically the chaotic experimental behavior, we compute and present in Fig. 6 the ''spectra'' of five numerical simulations using the experimental coefficients with different initial conditions. It can be observed that they essentially overlap the experimental ''spectra'' and that their global shapes are recovered. In particular, a good agreement is exhibited for small indexed modes that are the most energetic ones. Also, we show here that the remained experimental noise appears as a deviation in the ''spectra.'' This is clearly visible for Ω_r and Γ_i, especially for the less energetic modes (for large indices).

We conclude that the experimental and the computed spatiotemporal fields are nearly identical, their ''spectral'' signatures being the same. This proves that our inversion method, based on a biorthogonal decomposition applied in the proper mode space (the dispersion relation), is able to recover the values of the parameters of the model. As it uses a general projection procedure it can be implemented on other chaotic extended systems and associated models and consequently should lead to better analyses of experimental observations of space-time chaos.

[1] M. Zdravkovich, Trans. ASME: J. Fluids Eng. **99**, 618 (1977).
[2] K. S. Chang and C. J. Song, Int. J. Numer. Methods Fluids **11**, 317 (1990).
[3] P. Le Gal, I. Peschard, M. P. Chauve, and Y. Takeda, Phys. Fluids **8**, 2097 (1996).
[4] P. Le Gal, C. R. Acad. Sci., Ser. II: Mec., Phys., Chim., Sci. Terre Univers **313**, 1499 (1991).
[5] M. P. Chauve and P. Le Gal, Physica D **58**, 407 (1992).
[6] M. Provansal, C. Mathis, and L. Boyer, J. Fluid Mech. **182**, 1 (1987).
[7] J. Dusek, P. Le Gal, and Ph. Fraunié, J. Fluid Mech. **264**, 172 (1994).
[8] O. Cardoso, H. Willaime, and P. Tabeling, Phys. Rev. Lett. **65**, 1869 (1990).
[9] I. Peschard and P. Le Gal, Phys. Rev. Lett. **77**, 3122 (1996).
[10] N. Aubry, R. Guyonnet, and R. Lima, J. Stat. Phys. **64**, 683 (1991).
[11] J. M. Fullana, P. Le Gal, M. Rossi, and S. Zaleski, Physica D **102**, 35 (1997).
[12] J. M. Fullana and S. Zaleski, Phys. Rev. Lett. **79**, 3182 (1997).
[13] D. P. Vallette, G. Jacobs, and J. P. Gollub, Phys. Rev. E **55**, 4274 (1997).
[14] P. Le Gal, M. P. Chauve, I. Peschard, and S. Jarre, in *Current Topics in The Physics of Fluids, Research Trends*, edited by S. G. Pandalai (Research Trends, India, 1994), Vol. 1, p. 307.
[15] W. H. Press, S. A. Teukolsky, W. T. Vetterling, and B. P. Flannery, *Numerical recipes in C* (Cambridge University Press, Cambridge, England, 1992).